Group 2: Optimal Design of a Dishwasher

Christopher Turner
Sub-system 1: Piping

Francesca Suer
Sub-system 2: Heating

Seunghui Huh
Sub-system 3: Pump

Visakan Mathivannan
Sub-system 4: Spray Mechanism

***Abstract*— A dishwasher is a complicated kitchen appliance used to wash plates and utensils, commonly found in homes under the kitchen countertop. The aim of this project was to reduce the environmental impact of a dishwasher. This was achieved on a system level by minimising the cost throughout the lifetime of the dishwasher through reducing the energy consumption of the pump, friction losses in the piping, maximizing the efficiency of the heating element and maximizing the cleaning ability of the spray arms. The problem was split into four subsystems: piping, heating, pump, spray arms. This enabled each author to create models of their assigned subsystem before optimizing each part. Afterwards the models were combined to create a single unified optimization problem. This was solved using *SQP algorithm* yielding the result of £197.18 total cost.**

I. Introduction

A dishwasher is found in most modern homes and serves to wash dishes and utensils automatically. It sprays heated water from below the plates via two rotating spray arms which aim to evenly distribute the water with enough pressure to clean the items inside effectively. The objective of this system optimisation is to minimise the environmental impact of the dishwasher by reducing electricity and water consumption. The average dishwasher is used once a week and lasts for 9.5 years before being discarded [1]. Each subsystem considers its own trade-offs against environmental impact, including size and physical limitations to the material cost of certain components. The dishwasher cleaning process as a whole is very complex and difficult to model; thus, we have each focused on separate components of the system to optimise them to reduce losses.

II. System-Level Problem and Subsystem Breakdown

Minimise $f = cost_{pressure} + cost_{volume} + cost_{pipe} - \frac{T_i - T_0}{\left(\frac{\ln\left(\frac{r_B}{r_a}\right)}{2\pi L k_B} + \frac{\ln\left(\frac{r_c}{r_B}\right)}{2\pi L k_c} + \frac{1}{h*2\pi L r_c}\right)} + \beta\rho g * Q * \frac{H}{\eta} - 2I\sum_{i=1}^{i=n(2)}(\int(F_i D_i \sin\theta_i)dt)$

Subject to:

Subsytem 1 $(g_1 - g_{17}, h_1 - h_4)$

Subsystem 2 $(g_1 - g_7$

Subsystem 3 $(g_1 - g_8)$

Subsystem 4 $(g_1 - g_3, h_1, h_2)$

See individual subsystems for all constraints

Identical functions and variables are used in the subsystem formulations. Please refer to these for explanation and understanding of the functions and variables.

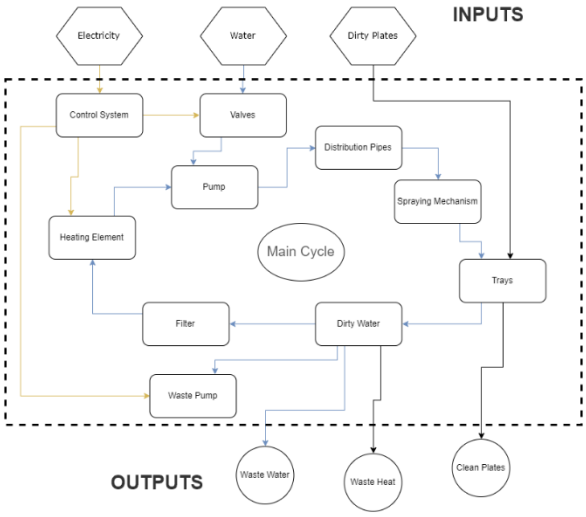

Figure 1: System level diagram

Dishwasher system diagram, Fig. 1, shows the links and flow between subsystems as well as the system boundaries.

III. Subsytem 1, Piping

The piping subsystem takes pressurised water from the pump in the base of the dishwasher and distributes it to the two spraying arms below the bottom and top trays. The objective of this optimisation was to reduce the pressure lost in the piping, reduce the volume of water required to fill the pipes and to reduce the cost of purchasing the piping to install in the dishwasher initially. The combination of these three enable us to minimise the cost of purchasing and running the dishwasher over its lifetime.

A. Optimisation formulation

Minimise $cost = cost_{pressure} + cost_{volume} + cost_{pipe}$

Subject to:

$$f_1 = cost_{pressure} - 6.3889 * \left(4 * f_0 * \frac{x_0}{D} * \frac{1}{2} * 997 * u_0^2 + 4 * f_1 * \frac{x_1}{D} * \frac{1}{2} * 997 * u_1^2 + 2969\right) = 0$$

$$f_2 = f_0 - \frac{0.25}{\left(\log\left(\frac{0.0015}{3.7 * D} + \frac{5.74}{Re_0^{0.9}}\right)\right)^2} = 0$$

$$f_3 = Re_0 - \frac{u_0 * D}{10^{-6}} = 0$$

$$f_4 = f_1 - \frac{0.25}{\left(\log\left(\frac{0.0015}{3.7 * D} + \frac{5.74}{Re_1^{0.9}}\right)\right)^2} = 0$$

$$f_5 = Re_1 - \frac{u_1 * D}{10^{-6}} = 0$$

$$f_6 = u_1 - \frac{u_0}{2} = 0$$

$$f_7 = \pi * \left(\frac{D}{2}\right)^2 * u_0 - 0.00015 = 0$$

$$f_8 = x_0 - x_2 - x_{eq0} - x_3 = 0$$

$$f_9 = x_{eq0} - x_{e0} * D + \frac{\pi}{2} * R_0 = 0$$

$$f_{10} = x_{e0} - 22.2126 * \left(Re_0 * \left(\frac{D}{R_0}\right)^2\right)^{0.7888} * Re_0^{-0.71438} = 0$$

$$f_{11} = x_1 - x_{eq2} - x_4 - x_{eq3} - x_5 - x_{eq1} - x_6 = 0$$

$$f_{12} = x_{eq1} - x_{e1} * D - \frac{\pi}{2} * R_1 = 0$$

$$f_{13} = x_{e1} - 22.2126 * \left(Re_1 * \left(\frac{D}{R_1}\right)/^2\right)^{0.7888} * Re_1^{-0.71438} = 0$$

$$f_{14} = x_{eq2} - 0.6 * D - 3 * D = 0$$

$$f_{15} = x_{eq3} - 0.2 * D - 3 * D = 0$$

$$f_{16} = cost_{volume} - 472{,}758 * \left(x_2 + x_3 + x_4 + x_5 + x_6 + \frac{\pi}{2} * (R_0 + R_1) + 4 * D\right) * \pi * \left(\frac{D}{2}\right)^2 = 0$$

$$f_{17} = cost_{pipe} - \left(x_2 + x_3 + x_4 + x_5 + x_6 + \frac{\pi}{2} * (R_0 + R_1)\right) * 264 = 0$$

$$g_1 = D - R_0 \leq 0$$

$$g_2 = D - R_1 \leq 0$$

$$g_3 = 0.200 - x_2 - R_0 - \frac{D}{2} \leq 0$$

$$g_3 = x_2 + R_0 + \frac{D}{2} - 0.300 \leq 0$$

$$g_4 = R_0 + \frac{3}{2}D - 0.075 \leq 0$$

$$g_5 = 2D - 0.10 \leq 0$$

$$h_1 = R_0 + \frac{3}{2}D + x_3 - 0.075 = 0$$

$$h_2 = R_1 + x_5 + \frac{3}{2}D - 0.400 = 0$$

$$h_3 = x_6 + R_1 - x_2 - R_0 = 0$$

$$h_4 = x_6 + R_1 - x_4 - \frac{3}{2}D = 0$$

$$g_6 = 0.200 - x_6 - R_1 + \frac{D}{2} \leq 0$$

$$g_7 = x_6 + R_1 + \frac{D}{2} - 0.300 \leq 0$$

$$g_8 = 0.200 - x_4 - D \leq 0$$

$$g_9 = x_4 + \frac{3}{2}D - 0.300 \leq 0$$

$$g_{10} = -D \leq 0$$

$$g_{11} = -R_0 \leq 0$$

$$g_{12} = -R_1 \leq 0$$

$$g_{13} = -x_2 \leq 0$$

$$g_{14} = -x_3 \leq 0$$

$$g_{15} = -x_4 \leq 0$$

$$g_{16} = -x_5 \leq 0$$

$$g_{17} = -x_6 \leq 0$$

The main value function is simplified, all the functions are within the constraints, specifically in functions $f_1 - f_{17}$. This is to aid with understanding and provide a simplified, easy to follow model of the subsystem. There are two different values for the Darcy friction factor as there are two different flow rates, as we assume the flow rates out of both outputs of the tee-piece are the same. f_1 shows a simplified equation for the friction loss in the three sectors of the piping. Functions f_2 and f_4 calculate the friction factor using the Swamee-Jain equation, whilst f_3 and f_5 are derived from the definition of Reynolds number. The flow is assumed to split evenly after tee-piece into equal volumetric flows, as shown in f_6, and the additionally equivalent length for the 90° bends is shown in f_{10} and f_{13} based on a 2008 paper by Spedding P.L., Bénard Emmanuel and Mcnally G.M.[2]. The equivalent length of the tee-piece through path and branch path, f_{14} & f_{15} are the total equivalent length, frictional equivalent length plus real length, of the water flow going straight through the pipe and branching off the pipe[3].The flow is assumed to be 0.1 L/s, f_7, and the chosen material for the piping is copper, with a surface roughness of 0.0015[4], f_2 & f_3, and cost of 400p/m[5], f_{17}. None of the components can have negative dimensions and the main body of the tee-piece must be in the back of the dishwasher, between 200-300 mm from the centre. Finally, the diameter of the pipe is assumed to be constant throughout the whole dishwasher and the bends are all exactly 90° with a constant radius.

B. Modelling approach

The model is derived from first principles using known equations and values along with physical measurements. A simplified theoretical model is then shown in Fig. 2.

The pump is in the centre at the bottom of the dishwasher, with the height between the centre lines of the pump and the upper spray nozzle pipe being 7.5 cm and the distance between the upper spray nozzle and the lower spray nozzle being equal to 40cm. Further explanation of this diagram can be found in the subsystem folder. Constraint f_1 is based off the standard friction loss in pipes equation while f_2 and f_4 are the Swamee-Jain approximation of the Colebrook equation, used to calculate the Darcy friction factor. The definition of Reynolds number is given in f_3 & f_5. At the tee-piece the flow is assumed to have split evenly in half, this is expressed in f_6, while the tee-piece is assumed to be three times the pipe diameter in length along the through path, and have a spur halfway along this length with a length equal to the pipe diameter.

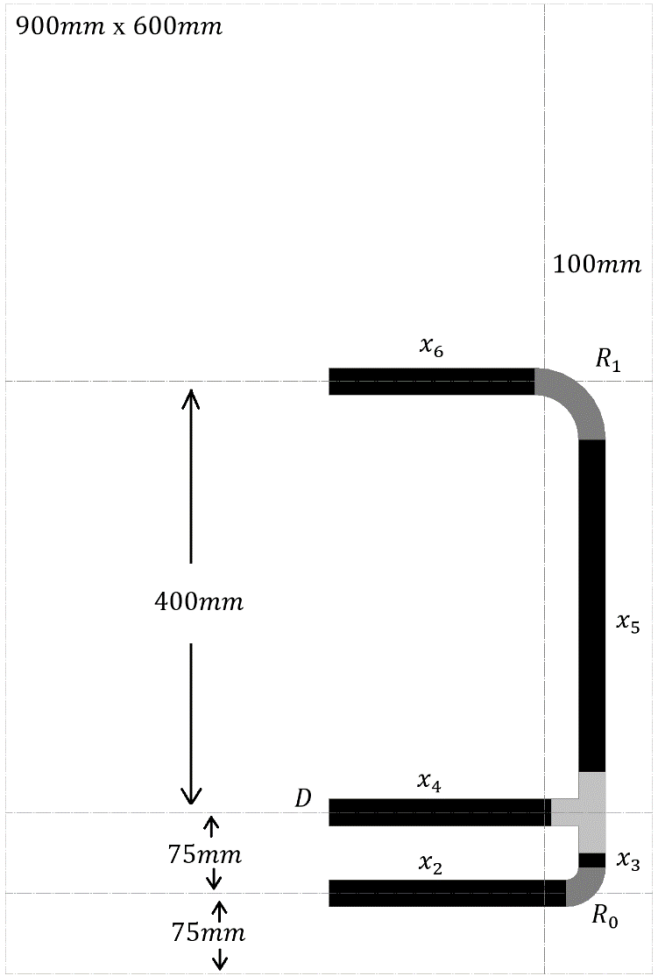

Figure 2: Interior Pipe Layout of a Dishwasher

With an assumed flow rate of 0.1 L/s f_7 expresses the average flow velocity as a function of the D. Functions f_{10} & f_{13} come from a paper[2] and express the equivalent lengths for a 90° bend based on pipe diameter D, bend radius R and Reynolds number Re. The equivalent length of features is their additional friction length f_{10}, f_{13} and the first halves of f_{14} & f_{15} plus their path length. This is shown is f_9, f_{12}, f_{14} & f_{15}. The costs, expressed in f_1, f_{16} & f_{17}, are based off average consumer prices[6][7][5]. This costing is because the aim of this subsystem optimisation is to reduce the waste costs throughout the lifetime of the product. Energy wasted due to pressure loss, excess water usage and material cost are the best way to do this. The lifetime of a dishwasher is assumed to be 9.5 year[1]**.** The back of the dishwasher is a cavity space within which the vertical piping must sit. It is 200-300 mm from the centre of the dishwasher and is designed to contain insulation and other components critical to the dishwasher. The piping is assumed cylindrical at all points, this has been proven to be the optimum cross-section for a pipe to reduce the hydraulic diameter for a given cross sectional area, see piping subsystem folder for further proof.

C. Explore the problem space

The problem is a convex, constrained, nonlinear multivariable function. The model was simplified to a two-dimensional shape after the additional third dimension gave too many variables and complications creating a standard model. All variables are bounded and thus the problem is well posed, and a meaningful optimum can be reached. Monotonicity analysis was performed and h_1, g_{12} & g_{13} are inactive, so have been removed from the formulation in MATLAB. It was found that while x_2, x_3, x_4, x_5, x_6, R_0 and R_1 are monotonic, D is not.

D. Optimise

The problem was optimised using MATLAB and two different algorithms in *fmincon*. Functions f_1 – f_{17} were placed inside the called value function as they are the functions that make up the value function and were listed separately here and in MATLAB to simplify the layout and user understanding. The active-set algorithm was used as it can take large steps between iterations, thus making it a faster algorithm to run when compared to something like interior-points. For the second attempt sequential quadratic programming was used as it satisfies all the bounds at each iteration, thus making for a more reliably feasible result. However, as it is not a very scalable algorithm it was used second under the anticipation it would take longer. The results of both are identical and found in Table 1.

Table 1: Optimal results of Piping Subsystem

x_2	x_3	x_4	x_5	x_6	R_0	R_1	D	$cost$
0.185	0	0.170	0.140	0	0.03	0.215	0.03	19,167.2

Drawn copper tube has a surface roughness between 0.001 x10^{-3} m and 0.002 x10^{-3} m. For the initial equation it was assumed the mean of these two number, 0.0015 x10^{-3} m, was the surface roughness. However, as the bounds show, this can change by up to 33%. The analysis was thus run again using the SQP algorithm for roughness values at 0.0001 x10^{-3} m intervals from and including 0.001 – 0.002 x10^{-3} m. During this, the value of the variables at the optimum point did not change. Additionally, the flow rate can change from 100 mL/s up to 200 mL/s. The average was used in the initial formulation to gain insight. Analysis has been run again with flow rates at 10 mL/s interval from and including 100 – 200 mL/s. The results of this showed no change in the optimal length, radius or diameter variables showing the subsystem is not sensitive to variations within the expected limits.

E. Discussion

Comparisons of the solutions of the two different algorithms showed they both had the same variable values and repeating the algorithm with a different starting point gave the same result. Contrary to expected behaviour, SQP ran quicker than the active-set algorithm, in around half the time. The active-set algorithm can take large steps between iterations, making it a faster algorithm to run compared to other constrained nonlinear multivariable algorithms. However, it is not a large-scale algorithm and thus is less computationally efficient for large scale problems than an algorithm like interior-points. The second algorithm chosen was SQP. SQP is also not considered a large-scale algorithm as it creates full matrices at each step and uses computes with dense linear algebra. Yet, SQP satisfies all its bounds at each iteration meaning each iteration produces a viable solution.

From the results it can be seen that x_3 and x_6 are both equal to 0, meaning they do not exist and are removed. This is an acceptable option as the curved pieces of piping can cover

the gap otherwise left. It was also expected because as the radius increases, the pressure lost due to the bending of the pipe decreases and the length of a curved pipe between two points is less than the length of two pipes that are perpendicular to each other and tangential to the curved pipe at the two points in space. Thus, the largest possible radius makes sense, and so the curved pieces will increase in size until they remove one of the linear pipes they join to, x_2 or x_3, and x_5 or x_6.

The design made several assumptions and improvements that would be interesting to analyse in the future. One of these is the splitting of the pipe into two. A simple tee-piece was used, however a more efficient fitting would be a gradual split, where the pipes then curve steadily away from each other, rather than a sudden 90° turn. Additionally, the curves have been assumed to be only 90° and the straights pipes only go vertically or horizontally, in the future, a different layout could be proposed that removes this simplification. Finally, the pipe was assumed to be constant diameter before and after the splitting. This meant that half the pressure loss from friction is lost before the splitting, despite only being 28% of the total pipe length. In the future, changing the assumption, to assume the pipe before can be a different diameter could lead to a different result and a more optimal value.

IV. Subsystem 2: Heating

This subsystem focuses on the heating of the dishwasher water. Dishwashers typically use one of two ways to heat water. One option is to use a flow through heater, these devices instantly heat water as it flows through the device into the dishwasher and require high power. Other dishwashers use a heating element that sits at the bottom of the dishwasher and heats the water once it has filled into the basin. I have chosen to optimise a heating element for this project because I believe it provides a more interesting optimisation problem. To optimise in terms of sustainability, the heating element must be as efficient as possible. This means maximising the heat flux (a measure of watts per square meter emitted) from the core of the element to the outside surface of the element for a given power supplied. The objective function and all constraint mathematical models have been derived from first principals.

A. Optimisation formulation

Model in negative null form:

Max $f(x) = q$

Min $-f(x) = -q$

$$= -\frac{T_i - T_o}{\left(\frac{\ln\left(\frac{r_B}{r_A}\right)}{2\pi L k_B} + \frac{\ln\left(\frac{r_C}{r_B}\right)}{2\pi L k_C} + \frac{1}{h 2\pi L r_C}\right)}$$

where variables, $\boldsymbol{x} = (L, M_B, r_A, r_B, r_C)$

and parameters, $\boldsymbol{p} = (T_i, T_o, M_C, M_A, R, h)$

s.t $g1(L)\colon L - 2.14 \le 0$

$g2(L)\colon 1.57 - L \le 0$

$g3(L, r_A)\colon R - \frac{\rho_A L}{\pi r_A^2} \le 0$

$g4(r_A, r_B, M_B)\colon \frac{230}{\varepsilon_B} - r_B + r_A \le 0$

$g5(r_B, r_C)\colon r_B - r_C + 4.5 \times 10^{-6} \le 0$

$g6(r_C)\colon r_C - 2.1 \times 10^{-2} \le 0$

$g7(r_B)\colon 2 \times 10^{-4} - r_B \le 0$

B. Modelling approach

Objective function derivation & assumptions

The heating element can be modelled as a cylinder comprising of multiple layers, each playing a different role Fig. 3. Layer A, the core, generates heat from a current flow. Layer B, the middle layer, provides electrical resistance. Finally, layer C, the outermost layer, provides corrosion resistance. Layer A's radius is represented r_A, layer B's r_B and layer C's r_C. The length of the pipe is represented as L and the surface temperature of layer A and layer C as T_i and T_o respectively.

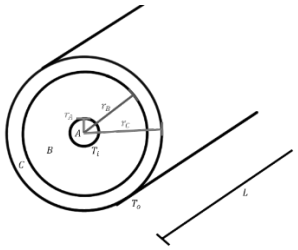

Figure 3: Diagram of the cross section of the heating element

Steady state heat transfer through a multi-layered pipe can be modelled according to Fourier's Law[8][9][10] as:

$$q = \frac{T_i - T_o}{R_{Total}}$$

Heat flux (q) is greater for a greater temperature gradient between the outside of the pipe (T_o) and the core (T_i). Equally, the greater the total thermal resistance (R_{Total}), the smaller the heat flux. The total thermal resistance is made up of three parts for this model, the thermal resistance due to conduction through layer B ($R_{conductionB}$), the thermal resistance due to conduction through layer C ($R_{conductionC}$), and the thermal resistance due to convection from layer C to the surrounding water ($R_{convectionC}$):

$$R_{Total} = R_{conductionB} + R_{conductionC} + R_{convectionC}$$

$$R_{conductionB} = \frac{\ln\left(\frac{r_B}{r_A}\right)}{2\pi L k_B}$$

$$R_{conductionC} = \frac{\ln\left(\frac{r_C}{r_B}\right)}{2\pi L k_C}$$

$$R_{convectionC} = \frac{1}{h 2\pi L r_C}$$

Therefore, $q = \frac{T_i - T_o}{\left(\frac{\ln\left(\frac{r_B}{r_A}\right)}{2\pi L k_B} + \frac{\ln\left(\frac{r_C}{r_B}\right)}{2\pi L k_C} + \frac{1}{h 2\pi L r_C}\right)}$

Several assumptions were made:

- T_o is the same temperature as the water outside the heating element.
- T_o does not change as the water heats up.
- No energy is lost to external surrounding.
- Heat is evenly distributed throughout the water from the heating element.
- Heat transfer via radiation has been ignored.

- The convective heat transfer coefficient of water (h) is equal to $1525 W/m^2K$[11].

Constraint derivation & assumptions

$g1(L)$ and $g2(L)$ ensure the length of the element is bounded from above and below so that it fits inside the dishwasher based on the average size of a dishwasher[12] and estimation of the size of parts found on the base of the dishwasher Fig. 4.

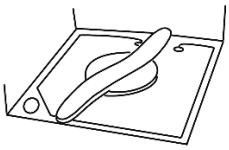

Figure 4: Diagram of the dishwasher base space

$g3(L, r_A)$ ensures the resistance of layer A generates sufficient power to heat the water. The power necessary (P) was calculated as follows:

$$P = \frac{\mathrm{mc}(T_i - T_o)}{t}$$

Assuming the mass of water (m) as $13kg$ per cycle[13], the specific heat capacity of water (c) as $3976.7 J/kgK$[14], the time taken for the water to be heated (t) as $120\,s$ [15], the temperature of the water fed into the dishwasher (T_o) is 328K[16] and the temperature of the water is heated to (T_o) 335.5K[17]. From the power output estimation, the total required electrical resistance of layer A (R) can be derived as follows:

$R = P/I^2$

Where the current draw (I) is derived from:

$I = P/V$

Where the voltage (V) is the UK mains value of 230V.

The resistance (R) of the core is equal to:

$$R = \frac{\rho L}{\pi r_A^2}$$

I have chosen nichrome as layer A's material because it is widely used in industry for this purpose due to its high electrical resistance and melting point, it has a resistivity (ρ) of $1.3 \times 10^{-6} \Omega m$ [18]. Equating the two electrical resistance equations that equal to R leads us to the inequality constraint $g3(L, r_A)$. $g4(r_A, r_B, M_B)$ ensures that the thickness of layer B ($r_B - r_A$) provides sufficient electrical resistance for a mains voltage of 230V. The dielectric strength of layer B (ε_B) is the maximum electric field the material can withstand at a given material thickness before undergoing electric breakdown where the material becomes a conductor. I have assumed dielectric strength is proportional to thickness for each material.

Using CES Edupack I generated a plot of thermal conductivity against dielectric strength, Fig. 5. It was clear that technical ceramics had most appropriate material properties. Within this material subset, I chose three materials that are used in industry, Table 2, with tradeoffs between dielectric strength and thermal conductivity to analyse in this optimisation study.

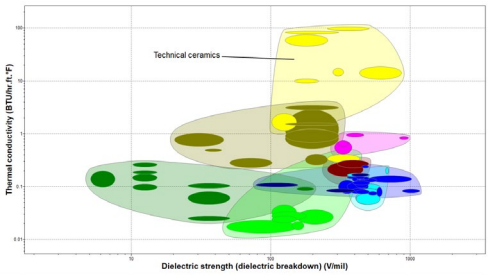

Figure 5: Plot of dielectric strength against thermal conductivity highlighting technical ceramics[19]

Table 2: Material Selection for Layer B

Material	Dielectric strength, ε_B (V/m)	Thermal conductivity, k_B (W/mK)
Mica	1420×10^3	5.92
Aluminia	726×10^3	13.46
Mullite	278×10^3	3.46

$g5(r_B, r_C)$ ensures the thickness of layer C, $(r_C - r_B)$ provides sufficient corrosion resistance for a life of 9.5 years[1]. I have chosen stainless steel as the material for layer C because it is widely used in industry for this purpose due to its high corrosion resistance at elevated temperatures, it has a corrosion rate of $0.5\times 10^{-7} m/year$ in water[20].

r_B and r_C are non-monotonic variables in the objective function, therefore bounds were set to ensure the variables were monotonic within the problem formulation. $g6(r_C)$ provides an upper bound for r_C ensuring the element can fit beneath the dishwasher spraying element, estimated as $2.1 \times 10^{-2} m$ based on visual inspection. $g7(r_B)$ provides a lower bound for r_B as $2 \times 10^{-4} m$ based on a sensible estimation.

C. *Explore the problem space*

Initial parametric study

By keeping all variables constant apart from one, a parametric study was performed to see which variables had a significant impact on the objective in order to determine which to keep as variables and which to change to parameters. I used the `plot` function on MATLAB to plot r_A, r_B, r_C k_B, $k_C$and L against the objective Fig. 6. I wanted to do a material study for just one of the layers, since k_C had less significance than k_B, I made material C (M_C) a parameter and kept material B (M_B) as a variable.

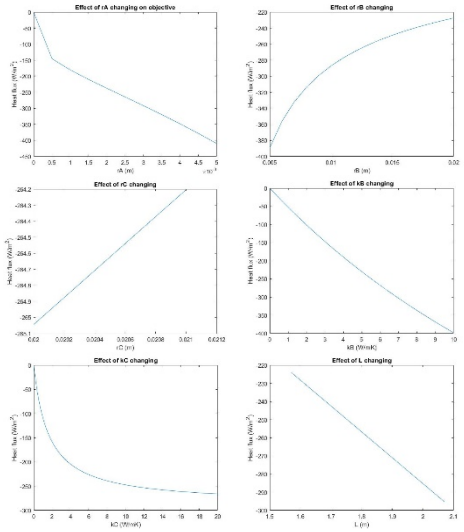

Figure 6: Initial Parametric study in MATLAB

Monotonicity analysis

From performing monotonicity analysis, Table 3, I identified that all constraints but $g2$ were active. Therefore, this constraint was removed. I have not included $g6$ or $g7$ in the monotonicity analysis because they provide bounds to ensure r_B and r_C are monotonic.

Note: The materials in Table 2 will determine k_B.

Table 3: Material Monotonicity Table

	L	r_A	r_B	r_C	k_B
$-f$	-	-	+	+	-
$g1$	+				
$g2$	-				
$g3$	-	+			
$g4$		+	-		
$g5$			+	-	

D. Optimise

Algorithms

I used gradient based constrained optimisation methods using the programming solvers on MATLAB to optimise the non-linear constrained problem. I used both `Fmincon` and `Global search`. Both solvers attempt to find the selection of variables that produce the lowest objective value. There are three algorithms that can be used within `Fmincon`: SQP (sequential quadratic programming), Active set and Interior Point. All algorithms converged to the same solution. SQP and Active set are small-scale algorithms and Interior point is large-scale because it can take large steps so was faster to run. It was clear all algorithms within `Fmincon` got stuck in a local minimum because the objective value found using `Global search` was an improvement from the others showing that it had found the global minimum, however this solver has a longer running time. It should be noted that it was important to have a good estimation of the initial point for the algorithms to work well.

The material generating the minimum objective value for each algorithm was Aluminia. `Global search` found a global objective minimum value of 290 W/m^2 for Aluminia. This is a 1317% improvement on the unoptimized problem. The results are shown in Table 4.

Table 4: Algorithm Results - Alumina

Algorithm	$q(W/m^2)$	Time (s)	r_A (m)	r_B (m)	r_C (m)	L (m)
SQP	279	0.0120	7.35×10^{-5}	3.90×10^{-4}	1.22×10^{-2}	2.14
Active Set	279	0.0163	7.35×10^{-5}	3.90×10^{-4}	1.22×10^{-2}	2.14
Interior Point	279	0.0358	7.35×10^{-5}	3.90×10^{-4}	1.22×10^{-2}	2.14
Global Search	290	1.29	7.35×10^{-5}	2.00×10^{-4}	1.22×10^{-2}	2.14

All solvers used an initial point of $x_0 = [0.00006, 0.0003, 0.0003, 1]$.

Post-optimality parametric study

To conduct a post optimality parametric study, I changed values of some of the parameters to see how they would affect the optimisation problem if they were instead variables. The initial temperature of water fed into the dishwasher (T_o) was changed to 280K which is the temperature of cold tap water, (rather than of hot tap water)[21]. This led to a large objective increase of 2435 W/m^2. The time for the element to heat the water (t) was doubled to 240 s and the mass of water to be heated (m) was halved to 7.5 kg both leading to an objective decrease of 97 W/m^2. From this, it was clear that the variation in T_o has a significant impact on the objective function so should potentially be changed to a variable, t and m are less significant so can remain parameters.

E. Multi-objective optimisation

I reformatted the problem to consider the influence of material B's embodied CO2. An additional objective was added to minmise the embodied CO2, (C).

$$Min\ f(x) = [\, f_1(x), f_2(x),] = [-q, C]$$

$$where\ variables,\ \boldsymbol{x} = (L, M_B, r_A, r_B, r_C, C_B)$$

$$and\ parameters,\ \boldsymbol{p} = (T_i, T_o, M_C, M_A, R, h)$$

$$f_1(x) = -q$$

$$= -\frac{T_i - T_o}{\left(\frac{\ln\left(\frac{r_B}{r_A}\right)}{2\pi L k_B} + \frac{\ln\left(\frac{r_C}{r_B}\right)}{2\pi L k_C} + \frac{1}{h 2\pi L r_C}\right)}$$

$$f_2(x) = C = m_B C_B$$

A range of data points at different thicknesses of layer B were passed through the objective function for each material to find the relationship between q and C with a pass/fail criteria applied to ensure the thickness was large enough to provide sufficient electrical resistance for a mains voltage of 230V to satisfy constraint $g4$. The values passed were plotted, Fig. 7, to see if a Pareto set formed, i.e. the objective is to maximise heat flux and minimise embodied CO2 and different materials may have presented tradeoffs between the two. A Pareto set did not form because all materials that generated a higher heat flux also generated a lower embodied CO2, therefore there was no tradeoff between the two objectives. However, this led to an obvious optimal point

represented by Aluminia with a heat flux value of $275 W/m^2$ and embodied CO2 of $2.66\times 10^5 J/kg$.

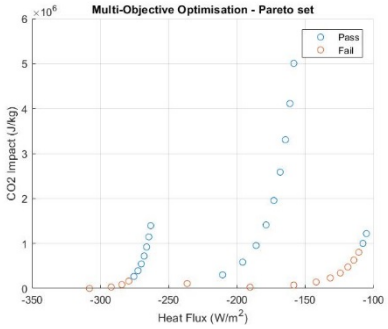

Figure 8: Heat flux vs embodied CO2

F. Discussion

This subsystem was successfully optimised, finding the minimised objective function and values for all variables to achieve this using `Global search`.

Initially, a parametric study was performed to identify variables that had a significant impact on the objective in order to set those that did not to parameters. Next, `Fmincon` was implemented with three algorithms (SQP, Interior Point and Active-set). These algorithms identified a minimum value for the objective, all converging to the same solution. However `Global search` identified an improved solution. Aluminia was identified as the material to generate the highest heat flux in all solvers. `Global search` identified the optimum as 290 W/m^2 Table 5. This is a 1317 % improvement on the unoptimized problem.

Table 5: Final Results - Alumina

$q(W/m^2)$	Time (s)	r_A (m)	r_B (m)	r_C (m)	L (m)
290	1.29	7.35×10^{-5}	2.00×10^{-4}	1.22×10^{-2}	2.14

Next, the problem was reformatted to a multi-objective problem where the embodied CO2 of material B was considered as well as heat flux.

The subsystem study was limited because of various assumptions and simplifications made. For example, layer A has been modelled as a cylinder but in practice it would be a coil embedded within layer B, this significantly alters r_A's relationship with L. Additionally, the dielectric strength of a material tends not to have a linear relationship with thickness, this affects $g4$. I attempted to use a simulation to model this relationship more accurately but there was not sufficient data available to do so. Furthermore, no safety factors were taken into consideration so all the determined thicknesses of each layer of the element were calculated as considerably smaller values than they would be in practice. Finally, it would be interesting to test the multi-objective function with further materials to see if a Pareto set would form to allow for designer choice input.

V. SUBSYSTEM 3: PUMP

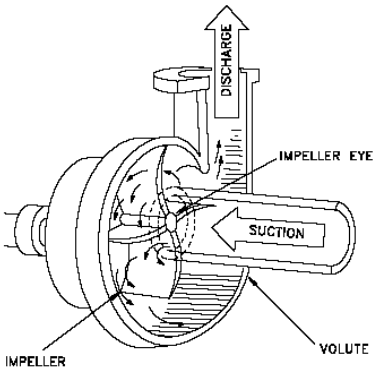

Figure 7: Centrifugal Pump Diagram

The third subsystem focused on is the pump. Among many pumps, the centrifugal pump has been chosen, for this type of pump is used mostly on dishwashers. A centrifugal pump is a mechanical device designed to carry fluid by the transfer of rotational energy through rotors called impellers. Fluid enters the rapidly rotating impeller along its axis and cast out by centrifugal force along its circumferences through the impeller's vane tips.

A. Optimisation Formulation

$$\textit{min} \quad f(\beta, P_{in}, P_{out}, r, v) = \beta\rho g * Q * H/\eta$$

$$\textit{where} \quad Q = \pi r^2 * v$$

$$H = (P_{out} - P_{in})/\rho g$$

$$\textit{s.t.} \quad g_1(P_{in}, P_{out}) = P_{in} - P_{out} + 25000 \leq 0$$

$$g_2(r, v) = -\pi r^2 * v + 0.001 \leq 0$$

$$g_3(P_{in}) = P_{in} - 125000 \leq 0$$

$$g_4(P_{out}) = -P_{out} + 125000 \leq 0$$

$$g_5(\beta) = -\beta + 0.95 \leq 0$$

$$g_6(\beta) = \beta - 1 \leq 0$$

$$g_7(r) = -r \leq 0$$

$$g_8(v) = -v + 4 \leq 0$$

The aim of the subsystem is to minimise the power input of the pump motor while maintaining the minimum consumption of power to clean dishes. The mathematical model was created to calculate the minimum power input of the pump. The cost of the

Variables were chosen based on the feasibility of changes: radius of the outlet of the pump r, pressure values at the inlet/outlet of the pump, fluid velocity, and volumetric temperature coefficient.

$$\text{Variables: } \beta, P_{in}, P_{out}, r, v$$

Constraints were applied based on scientific research to avoid any potential flaws for optimisation. For example, if the inlet pressure is higher than outlet pressure, a phenomenon called cavitation occurs[22].

Figure 9: Cavitation of a Pump

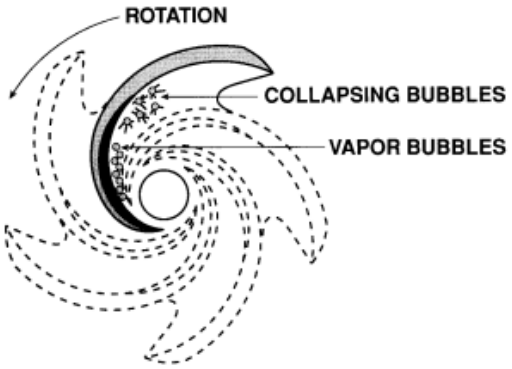

The drop of pressure causes bubbles to form, which "strike" impellers and damage them as shown in Fig. 9. The phenomenon significantly drops the efficiency of the pump, thus must be avoided. Another constraint, the minimum value of flow rate to clean dishes, was extracted from the Bosch report[23]. Refer to the constraints table for further descriptions presented in Table 6.

Table 6: Constraints Description Table

g_x	Description
g_1	Minimum pressure difference of inlet and outlet of the pump
g_2	Minimum flow rate that pump need to produce
g_3	Minimum pressure value at pump inlet
g_4	Maximum pressure value at pump outlet
g_5	Minimum value of the volumetric temperature coefficient
g_6	Maximum value of the volumetric temperature coefficient
g_7	Minimum outlet pipe radius value
g_8	Minimum fluid velocity at the outlet of pump

Design parameters were considered to make the outcome more realistic. Refer to the model parameters table for exact values presented in Table 7.

Table 7: Parameters Description Table

Gravity acceleration: g	9.81 m/s^2
Water density at 4°C: ρ	1000 kg/m^3
Efficiency value of typical pump: η	0.7 dimensionless

Due to the high complexity of fluid dynamics, many systemic assumptions were made to simplify the optimisation and validify the mathematical model. These assumptions are not part of the constrictions but considered to validate the mathematic equation. A list of assumptions is laminar flow, uniform density of fluid, momentum conserved, and energy conservation.

B. Modelling Approach

The mathematical model has been derived from the first principles[24]. Though, validation for several variations was taken place before applied to the mathematical model.

Using the projectile equation, output fluid velocity that can reach 0.8m height of dishwasher was calculated.

$$\text{Height} = v^2/2g$$

From the equation, the minimum value for velocity was determined. With the velocity value, the minimum value for the radius of the outlet pipe was determined using the flow rate equation.

Volumetric temperature coefficient (VTC) is a value that changes depending on the temperature of the water. The volumetric temperature coefficient describes how dense the liquid is and how it affects the viscosity of the fluid. For the optimisation, the temperature of 65 °C was used: this value is the most frequently used temperature for dishwashers. VTC value was extracted from the VTC chart, which is provided below in Fig. 10.

Figure 10: ß Value vs Temperature

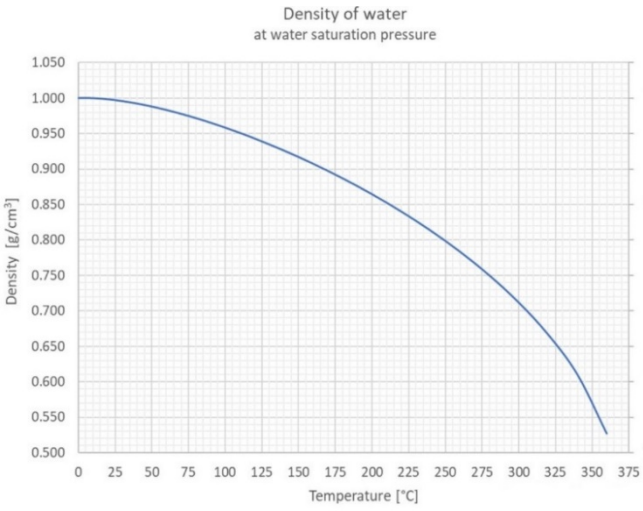

Cavitation was the major constraint of the subsystem. Due to the constraint, a specific value of the difference of inlet pressure and outlet pressure had to be set using the data below in Fig. 11. Like the VTC, the value changes depending on the temperature. So, to produce consistent outcomes, the temperature was set to 65 °C.

Figure 11: Minimum Pressure Difference to Avoid Cavitation

Temperature (°C) (deg F)	Vapor Pressure (kPa, kN/m²) (psi)
0	0.6
5	0.9
10	1.2
15	1.7
20	2.3
25	3.2
30	4.3
35	5.6
40	7.7
45	9.6
50	12.5
55	15.7
60	20
65	25
70	32.1
75	38.6
80	47.5
85	57.8
90	70
95	84.5
100	101.33

Subsystem Assumptions:

- The minimum inlet pressure must be higher than 100 kPa (1 bar).
- The maximum outlet pressure must be lower than 150 kPa (1.5 bar).
- The radius of the outlet pipe is larger than 0 mm.
- Dishwasher height is 0.8 m.
- Fluid velocity must be a positive number

C. *Explore the Problem Space*

To minimise and analyse the problem, monotonicity table was created as presented in Table 8. Using the constraints activity, the inactive constraint was removed from system.

Table 8: Monotonicity Table

	β	P_{in}	P_{out}	r	v	type
f	+	+	−	+	+	N/A
g_1		−	+			Semi
g_2				−	−	Semi
g_3			+			Active
g_4		−				Active
g_5	−					Active
g_6	+					Inactive
g_7				−		Active
g_8					−	Active

Figure 12: Visualisation of Bernoulli equation

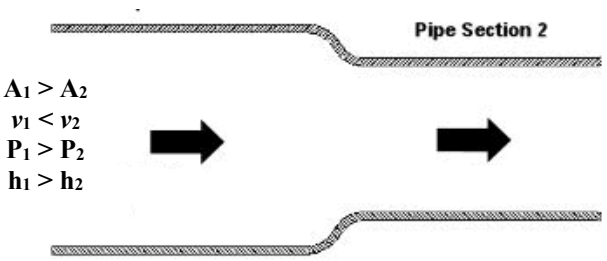

$$\rho v_1^2/2 + P_1 + \rho g h_1 + H_{pump} = \rho v_2^2/2 + P_2 + \rho g h_2$$

Bernoulli's equation

According to Bernoulli's equation, there is a relationship between pressure, a radius of the pipe, and fluid velocity. As shown in Fig. 12, narrower pipe results in higher fluid velocity, but lower fluid pressure. Because of the two constraints, the minimum fluid velocity and cavitation, several considerations took place before implementing values to the mathematic equation. Both minimum fluid velocity and minimum pressure difference due to cavitation have set values. So, in order to simplify the problem, the pump system was calculated with the same inlet & outlet pipe radius and equal fluid velocity at both the inlet & outlet of the pump. Setting these values equally simplifies the role of the pump: increasing the outlet pressure to avoid cavitation

D. *Optimise*

In order to obtain a tentative result of the local minima of the mathematic function, MATLAB algorithm *fmincon* was used. *Fmincon* algorithm was used for its fast implementation for solving nonlinear problems. Results are presented in Table 9.

Table 9: Results from Interior Point Algorithm

β	P_{in}	P_{out}	r	v	Power output
0.95	125kPa	150kPa	0.009m	4m/s	34.54 watt

Although *fmincon interior point* is a useful algorithm, it has a limitation: it can solve for a local minimum, which does not necessarily mean global minima. In order to obtain a more accurate and reliable result, *fmincon sqp* algorithm was also used and presented in Table 10. Both algorithms result consistent outcomes.

Table 10: Results from SQP Algorithm

β	P_{in}	P_{out}	r	v	Power output
0.95	125kPa	150kPa	0.009m	4m/s	34.54 watt

E. *Discussion*

Using the MATLAB algorithms *fmincon* and *fmincon sqp,* required power of 34.54 watt was obtained. Considering that usual power required for centrifugal pump of dishwasher is around 200 watts[25], the optimised value is about 7 times lower, which is highly unrealistic. The main reason for the result is due to the systematic assumptions. Centrifugal pump

inevitably creates vortex and turbulent flow, when transferring mechanical energy to pressure increase. This phenomenon takes huge element that decreases efficiency of the pump[26]. Yet, the both optimisation algorithms produced consistent outcomes, and the method to minimise power output using the constraints can reduce significant power requirement for centrifugal pump.

Using the result, cost for life-time usage was calculated by multiplying 90 (min) * 52 (weeks) * 7 (year) * 14.37 (pence) / 1000 (per kWh). The original cost would have been 941.5 pounds, but the optimised value results 162.6 pounds, which then the savings would theoretically be 779 pounds.

VI. Subsystem 4: Spray Mechanism

The spray mechanism is the subsystem that controls the behaviour of flow, from when it enters the spray arm to it hitting the load. This optimisation problem revolved around mathematically modelling and calculating the optimal configurations of the spray arm in order to create the most efficient flow of water and coverage of the load. Within this problem it is important to note that the cleaning process itself is not a well understood system [27] and that due to uncontrollable nature of humans and the way that the load would be arranged having a full understanding of coverage is also difficult.

Currently dishwashers aim to achieve maximum coverage by varying pressures of the pump to create different trajectories within the jets and focus on using a combination of a minimum temperature and pressure in order to ensure that the load is clean [27]. Therefore, the optimisation of this system focuses on maximising the angular velocity of the spray arm in order to create a larger coverage of the system by allowing for a bigger range of jet velocities and configurations of nozzles. This ultimately increases the efficiency of the clean for given temperatures and pressures and indirectly reduces the environmental impact.

A. Optimisation Formulation

Model in negative null form:

$\max f_1(x) = \omega$

$\min f_1(x) = -\omega$

$$\omega = 2I \sum_{i=1}^{i=n(2)} \left(\int (F_i D_i \sin\theta_i) dt \right)$$

$$F_i = \frac{\rho\pi}{2n}\left(v_p^2 r_h^2 - \omega v_p r_h^3\right)$$

$$D_i = (D_s(i-1) + D_O)$$

where:

$$x = (\boldsymbol{\theta_i}, \boldsymbol{n}, \boldsymbol{r_h}, \boldsymbol{D_s}, \boldsymbol{D_o}, \boldsymbol{v_p})$$

$$p = (\boldsymbol{\rho}, \boldsymbol{I})$$

subject to:

$$h_1(\boldsymbol{n}, \boldsymbol{r_h}, \boldsymbol{D_s}, \boldsymbol{D_o}): 0 = \frac{L_b - r_h}{2} - D_e - (D_s(n-1) + D_o)$$

$$h_2(\boldsymbol{\theta_i}, \boldsymbol{v_p}): 0 = -p_w + \left(v_p \sin\theta\right)^2$$

$h_3(\boldsymbol{n}): n \in \mathbb{N}$

$$g_1(\boldsymbol{\theta_i}, \boldsymbol{v_p}): 0 < \left(\frac{-\left(v_p \cos\theta_i\right)^2}{2g}\right) + h_p$$

$$g_2(\boldsymbol{r_h}, \boldsymbol{v_p}): 0 < v_p \pi r_h^2 - Q_s$$

$$g_3(\boldsymbol{D_o}): 0 < D_o - 0.1$$

$$g_4(\boldsymbol{\theta_i}): 0 < 90 - \theta_i$$

$$g_5(\boldsymbol{\theta_i}): 0 < \theta_i$$

where:

$$p = (\boldsymbol{L_b}, \boldsymbol{D_e}, \boldsymbol{g}, \boldsymbol{h_p}, \boldsymbol{L_s},)$$

B. Modelling Approach

Objective function derivation:

The objective function was derived mathematically using a series of assumptions. The first major assumption is that the spray arm can be modelled like a rod, which can be used with to calculate both I and the volume of water using the equations below.

$$I = \frac{1}{12} m L_b^2$$

$$V_b = h_b w_b L_b$$

Other assumptions relevant to the rod include that the mass of the spray arm is negligible as most of the mass results from the volume of water held in the arm.

Furthermore, it is also assumed that each nozzle can be modelled as a jet of water with a corresponding reaction force. These jets are angled from the vertical to create a horizontal component producing a moment on the spray arm and this moment is relative to each nozzle due to differing values of D_i. The forces from these jets, which were derived using Bernoulli's principles, also took into consideration the spray arm's current angular velocity creating an iterative optimisation problem [27].

$$F_i = \rho Q_i (v_p - v_a)$$

$$\tau = F_i D_i$$

Each of these moments would then be summed together and doubled to consider both sides of the spray arm and multiplied by I to provide an angular acceleration in accordance with the following formula.

$$\alpha = \tau I$$

This angular acceleration was then integrated to calculate the resultant angular velocities and complete the objective function.

Constraints derivations & assumptions:

The constraints were derived from design principles and mathematically. h_1 is related to the blades length and design and states that the nozzles must be a set distance from both the center and ends and should be evenly separated regardless of how many holes there were. Both h_2 and $g_1$were derived from linear motion and define the key constraints to ensure minimum coverage is reached both in terms reaching the maximum height of the load (h_p) within the load seperation distance (p_w) .

The g_3 constraint was required to limit the maximum flow rate that exits the spray arm because the pump would have a

maximum pressure output. Finally g_4 and g_5 provide bounds for the nozzle angles to ensure that the force all acts in the same direction

Euler's iterative method:

This problem formulation is dependant upon changing values of omega and resulted in requiring an iterative solver in order to consider the step changes in angular velocity.
To resolve this Euler's method was applied until the angular acceleration stabilised and a constant angular velocity was achieved. This is represented by figure 10 demonstrating the eventual lack of acceleration. This plot was used throughout to validate the model was working correctly.

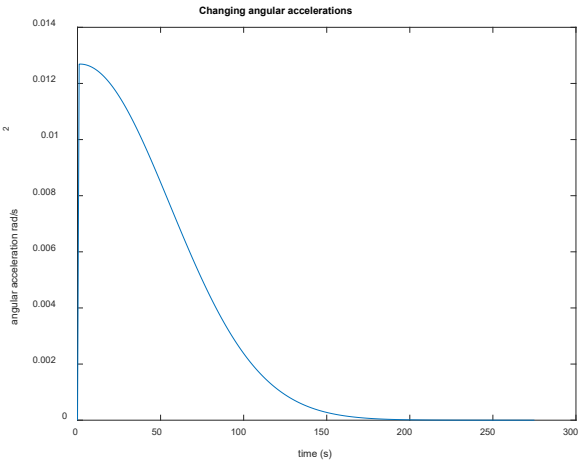

Figure 10:Graph showing angular acceleration stabilising

C. Explore the Problem Space

Monotonicity

In order to simplify the problem and ensure the variables are sufficiently constrained a regional monotonicity table was used where the objective function only focuses the regions defined by g_4 and g_5.

Table 11: Monotonicity table analysis for relaxing constraints

	θ_i	n	r_h	D_s	D_o	v_p
$f_1(x)$ **st**: g_3, g_4	-	-	+	-	-	-
h_1		+		+	+	
h_2	+					+
g_1	+					+
g_2			-			
g_3					+	

Using this monotonicity analysis g_3 is identified as an active constraint and can be substituted for D_O during the optimisation.

D. Optimise

The outlined problem having been simplified through monotonicity analysis and constraint relaxing resulted in a nonlinear optimisation problem. The initial steps taken to solve this was to use an interior point optimisation method within MATLAB. This ensured having the highest probability of finding a minimum as long as the problem was constrained correctly. Following this it became clear that the problem had a series of local minima because with different initial starting point the output value would change.

Therefore, a global search algorithm was used to identify the global minima, this is more computationally heavy but would more consistently provide a minimum value of approximately 18 $rad\ s^{-1}$. Using this set of starting values as initial values a more accurate set of values can be discovered using the `sqp` option of `fmincon` within MATLAB. This method is very similar to the Newton-Raphson method and is usually less computationally intensive and less effective at finding the correct solution. However, when combined with a good starting value, the accuracy is significantly improved, allowing identification of a optimal set.

The key issue with the current optimisation method was that the number of holes should be defined as a real integer but this was a condition that fmincon could not handle. Therefore, a variation of the problem was proposed where number of holes was moved to be a parameter and was solved again similarly. The resultant values are shown on table 13.

Table 12: Resulting angular velocities from varying integer values of n

n	4	5	6	7	8	9	10
$f(x)$	18.7	15.0	12.5	10.7	9.4	8.3	7.5

It was important to discretise this data because the algorithm is designed to deal with continuous data. However due to the nature of how the data was discretised the optimal value is clearly remaining approximately the same and n can now be considered a parameter.

E. Discussion

Algorithm

The key algorithms used for this optimisation was a global search algorithm alongside gradient based methods. The key difference identified related to computational efficiency and accuracy.

Initially use of gradient based methods such as interior point and SQP allowed for quick identification of different local minima. The problem could then be further solved by simplifying the problem through monotonicity analysis and analysing the constraints to find the ideal starting points for the algorithm. However, in the instance that problem was more complex with more variables it would be difficult to find the optimal starting point without some form of trial and error. Therefore, a global search method was used to identify the global minima points alongside the values for the design variable that reached this global minimum. Using this it was possible to then further improve the accuracy of the global search through the use of SQP, with it being designed to be effective with smaller scale algorithms.

Further testing was done to validate this was the best method of the three gradient based methods incorporated in

MATLAB. This involved testing each algorithm with randomised values and assessing how quickly the algorithm found the value and how accurate it was. Tests were also ran to see the effectiveness of the algorithm with well-defined starting points and the results are shown in table 14 and 15.

Table 13: Results showing average angular velocities and running time to solve for a randomised starting point

	Interior Point	SQP	Active set
Mean omega	-18.5579	-14.9657	-17.7475
Mean Time	0.2123	0.0712	0.1293

Table 14: Results showing average angular velocities and running times to solve after conducting a global search

	Interior Point	SQP	Active set
Mean omega	-18.6922	-18.6930	-18.6932
Mean Time	0.074	0.0239	0.251

It is shown that Active set was the more reliable but SQP was sufficiently accurate and the most computationally efficient from the starting point defined by the global search thus validating the decision to use it.

Sensitivity analysis

Having calculated the optimal values for a problem with 4 holes in each blade it is now possible to use the Active-set algorithm to accurately determine how each of the other design variables affect the output value. MATLAB was used alongside a series of `for loops` and `plot` functions to create a set of graphs for the changing design variables. Note that design variables D_s and D_o were found to be too constrained by h_1 and $g_3$and therefore the graphs for these were not included due to the optimisation problem failing to run.

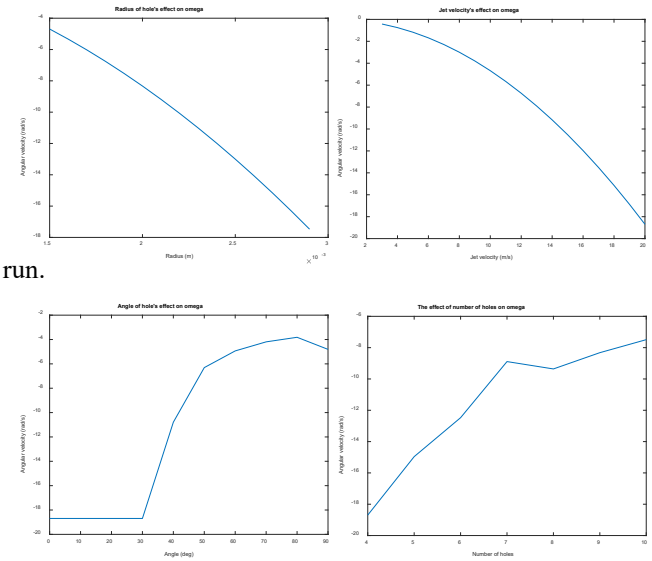

Figure 11: Graphs showing discretised changes to each relevant variable

From this sensitivity analysis as shown in figure 11 all four variables have a similar range of effects with slight differences. One of the key differences show was that number of holes had the smallest overall improvement on the subsystem. It was also interesting to note the effect of the angle of the hole which plateaus at its highest angular velocity. This allows the design to have some variation for its optimal configuration. Finally, the jet velocity has the potential to have the largest impact on the angular velocity and should require further analysis.

The last difference is particularly interesting from a system level perspective because it shows that the design variable, pressure, has the potential to significantly affect the spin rate and is the variable that has the most significant effect upon the environmental impact. Therefore in the future it would be good to separate the variable out and create a multiobjective function focusing on minimising pressure and maximing angular velocity.

Ultimately this subsystem was successfully optimised to provide the values in table 17 demonstrating angular velocity can be optimised but due to the nature of the problem it is difficult to turn this into a cost function and will act as a separate section to system level optimisation.

Table 15: Resulting set of x value and omega values from optimisation

θ_i	n	r_h	D_s	D_o	v_p	$f_1(x)$
25.3	4	0.003	0.066	0.00188	20	-18.693

VII. Conclusion

By deriving the monetary value of each subsystem in the dishwasher model, we were able to easily combine our subsystems into a coherent system overview. Additionally, the lack of interdependency between subsystems meant that they were able to be separated from each other, enabling us to each work on the subsystems separately, before combining them. Combining the systems together, in MATLAB we then ran the SQP algorithm in *fmincon*. This yielded a total cost of £197.18, which could be further improved upon. The cost of energy in the heating is £1.83, showing it to be a highly optimised system. Part of this may be due to the simplified nature of the model. The pump was the next efficient using only £3.68 of electricity during the lifetime of the dishwasher. Finally, the piping system wastes £191.67 of resources during its lifetime. This was expected to be the highest as the pipe is assumed to be wasted at the end of the life, the water stored inside the pipe is considered useless and it is impossible, outside of quantum mechanics, to get a fluid flowing without resistance. Subsystem 4 was omitted from this value as it's total cost is so small as to be negligible. This is due to it being a passive system.

In conclusion to our results, they approximate we expected them to be and the models make reasonable sense. The models were heavily simplified versions of their real-life counterparts and this most likely played a large part in the accuracy of our results.

VIII. NOMENCLATURE

1) Subsystem 1

D	Diameter of the pipe (m)
F_0	Darcy friction factor before tee-piece
F_1	Darcy friction factor after tee-piece
Re_0	Reynolds number of the initial flow
Re_1	Reynolds number of the flow after tee-piece
x_0	Equivalent frictional length from pump to the tee-piece (m)
x_1	Equivalent frictional length of tee piece and sections 2&3 (m)
x_2	Length of the bottom straight segment (m)
x_3	Length of straight segment before tee-piece (m)
x_4	Length of straight segment from tee-piece to bottom spray arm (m)
x_5	Length of straight segment from tee-piece to upper curved segment (m)
x_6	Length of straight segment from upper curved segment to upper spray arm (m)
x_{e0}	Equivalent length of resistance from the lower curved segment (m)
x_{e1}	Equivalent length of resistance from the upper curved segment (m)
x_{eq0}	Total equivalent length of lower curved segment (m)
x_{eq1}	Total equivalent length of the upper curved segment (m)
x_{eq2}	Total equivalent length of the path through the tee-piece (m)
x_{eq2}	Total equivalent length of the path branching off a tee-piece (m)
u_0	Initial flow velocity (m/s)
u_1	Flow velocity after tee-piece (m/s)

2) Subsystem 2

L	Length of the heating element (m)
M_A	Material A(N/A)
M_B	Material B(N/A)
M_C	Material C(N/A)
r_A	Radius of layer A (m)
r_B	Radius of layer B (m)
r_C	Radius of layer C (m)
T_i	Outside surface temperature of layer A (K)
T_o	Outside surface temperature of layer C (K)
R	Resistance(Ω)
h	Convective heat transfer coefficient of water (W/m^2K)
C	Embodied CO2 (J/kg)
C_B	Embodied CO2 of layer B (J/kg)
k_B	Thermal conductivity of layer B (W/mK)
k_C	Thermal conductivity of layer C (W/mK)
m	Mass of water heated (kg)
c	Specific heat capacity of water (J/kgK)
P	Power of the heater (W)
t	Time for the water to be heated (s)
I	Current (A)
V	Mains voltage (V)
ρ	Resistivity of layer A (Ωm)
ε_B	Dielectric strength of material B (V/m)

3) Subsystem 3

β	Volumetric temperature coefficient (dimensionless)
P_{in}	Pressure of the inlet of pump (kPa)
P_{out}	Pressure of the outlet of pump (kPa)
r	Radius of outlet of pipe of pump (m)
v	Fluid velocity at the outlet of pump (m/s)
Q	Flowrate at the outlet of pump (m^3/s)
H	Head value of pump ($Pa*s^2$ / $g*m^3$)

1) Subsystem 4

ω	Angular velocity of spray arm (rad/s)
I	Moment of Inertia of spray arm (kg m^2)
var_i	Variable in relation to i^{th} nozzle (dimensionless)
F	Reaction force of jet (N)
D_i	Position of i^{th} nozzle relative to centre (m)
θ	Angle between vertical of jet and spray arm
n	Number of nozzles (dimensionless)
ρ	Variable in relation to i^{th} nozzle (kg/m^3)
v_p	Velocity of water leaving jet (m/s)
r_h	Radius of nozzle (m)
D_s	Separation between each nozzle (m)
D_O	Offset distance of first nozzle from centre (m)
L_b	Spray arm length (m)
D_e	Maximum offset at the end of the spray arm (m)
p_w	Separation width of between plates (m)
h_p	Plate height (m)
Q_s	Max volumetric flow rate through spray arm (L/s)
m_b	Mass of spray arm (kg)
V_b	Volume of spray arm (m^3)
h_b	Height of spray arm (m)
w_b	Width of spray arm (m)
τ	Torque due to jet (Nm)
α	Angular acceleration of spray arm (rad/s^2)

REFERENCES

[1] Sprague G. How Long Should a Dishwasher Last on Average? [Internet]. Homeguides.sfgate.com. 2018 [cited 12 December 2019]. Available from: https://homeguides.sfgate.com/long-should-dishwasher-last-average-91045.html

[2] Spedding P, Bénard E, Mcnally G. Fluid Flow through 90 Degree Bends. Asia-Pacific Journal of Chemical Engineering [Internet]. 2008 [cited 1 December 2019];12(1-2):119. Available from: https://oatao.univ-toulouse.fr/20040/

[3] Pressure Loss from Fittings – Equivalent Length Method – Neutrium [Internet]. Neutrium.net. 2019 [cited 16 November 2019]. Available from: https://neutrium.net/fluid_flow/pressure-loss-from-fittings-equivalent-length-method/

[4] Roughness & Surface Coefficients [Internet]. engineeringtoolbox.com. 2003 [cited 6 December 2019]. Available from: https://www.engineeringtoolbox.com/surface-roughness-ventilation-ducts-d_209.html

[5] Wednesbury Copper Pipe 3m [Internet]. cityplumbing.co.uk. 2019 [cited 4 December 2019]. Available from: https://www.cityplumbing.co.uk/Wednesbury-Copper-Pipe-28mm-x-3m/p/701953

[6] Compare Energy Prices Per kWh | Gas & Electric Per Unit | UKPower [Internet]. Ukpower.co.uk. 2019 [cited 11 December 2019]. Available from: https://www.ukpower.co.uk/home_energy/tariffs-per-unit-kwh

[7] What does a litre or cubic metre of water cost? [Internet]. Unitedutilities.com. 2019 [cited 2 December 2019]. Available from: https://www.unitedutilities.com/faq/bills-payments/what-does-a-litre-or-cubic-meter-of-water-cost/

[8] YouTube [Internet]. Youtube.com. 2019 [cited 26 October 2019]. Available from: https://www.youtube.com/watch?v=PkcGgaxujJg

[9] YouTube [Internet]. Youtube.com. 2019 [cited 26 October 2019]. Available from: https://www.youtube.com/watch?v=Yfu-YVu2NKs&t=74s

[10] YouTube [Internet]. Youtube.com. 2019 [cited 26 October 2019]. Available from: https://www.youtube.com/watch?v=D78wOJvzCsY&t=322s

[11] Convective Heat Transfer [Internet]. Engineeringtoolbox.com. 2019 [cited 31 October 2019]. Available from: https://www.engineeringtoolbox.com/convective-heat-transfer-d_430.html

[12] Kitchens.com - Dishwashers - Dishwasher Sizes - Built-In Sizes [Internet]. Kitchens.com. 2019 [cited 31 October 2019]. Available from:https://www.kitchens.com/blog/products/dishwashers/mHY58K/dishwasher-sizes-built-in-sizes

[13] Christie S. Dishwasher vs washing up: which is cheaper? [Internet]. Telegraph.co.uk. 2019 [cited 3 November 2019]. Available from: https://www.telegraph.co.uk/finance/personalfinance/energy-bills/11250403/Dishwasher-vs-washing-up-which-is-cheaper.html

[14] Water - Specific Heat [Internet]. Engineeringtoolbox.com. 2019 [cited 3 November 2019]. Available from: https://www.engineeringtoolbox.com/specific-heat-capacity-water-d_660.html

[15] Dishwasher Normal Run Time [Internet]. Products.geappliances.com. 2019 [cited 3 November 2019]. Available from: https://products.geappliances.com/appliance/gea-support-search-content?contentId=18914

[16] [Internet]. 2019 [cited 14 November 2019]. Available from: https://www.ciphe.org.uk/consumer/safe-water-campaign/hot-water-scalds/

[17] All You Need To Know About Dishwasher Programs [Internet]. Dishwasherreviews.co.uk. 2019 [cited 20 November 2019]. Available from: http://dishwasherreviews.co.uk/need-know-dishwasher-programs.html

[18] Resistivity of Nichrome - The Physics Factbook [Internet]. Hypertextbook.com. 2019 [cited 21 November 2019]. Available from: https://hypertextbook.com/facts/2007/HarveyKwan.shtml

[19] CES Edupack 2019. Cambridge: CES; 2019.

[20] [Internet]. 2019 [cited 29 November 2019]. Available from: https://www.researchgate.net/figure/Corrosion-rate-of-aluminium-alloy-mm-year_tbl4_261567090

[21] [Internet]. 2019 [cited 29 November 2019]. Available from: https://www.quora.com/What-is-the-normal-temperature-of-tap-water

[22] Kim M, Jin H, Chung W. A Study on Prediction of Cavitation for Centrifugal Pump [Internet]. Semanticscholar.org. 2019 [cited 12 December 2019]. Available from: https://www.semanticscholar.org/paper/A-Study-on-Prediction-of-Cavitation-for-Centrifugal-Kim-Jin/3f1da789c831a2c8297dcb75295b4ab1a84ca161

[23] [Internet]. Media3.bosch-home.com. 2019 [cited 11 December 2019]. Available from: https://media3.bosch-home.com/Documents/9000157090_A.pdf

[24] Black H. Effects of Hydraulic Forces in Annular Pressure Seals on the Vibrations of Centrifugal Pump Rotors - H. F. Black, 1969 [Internet]. SAGE Journals. 2019 [cited 12 December 2019]. Available from: https://journals.sagepub.com/doi/abs/10.1243/jmes_jour_1969_011_025_02?casa_token=QV4Hyv3CA7wAAAAA:HGL-9PMVjpzeR8m5P8W4AmaRMo3HY_k3FjHiYwIaynNp54p8xtnDtLb6rfm9wOT1iUkXk0u1aNwp6w

[25] Power Consumption of Typical Household Appliances [Internet]. Daftlogic.com. 2019 [cited 12 December 2019]. Available from: https://www.daftlogic.com/information-appliance-power-consumption.htm

[26] Gulich J. Effect of Reynolds Number and Surface Roughness on the Efficiency of Centrifugal Pumps [Internet]. 2019 [cited 12 December 2019]. Available from: https://asmedigitalcollection.asme.org/fluidsengineering/article-abstract/125/4/670/439476

[27] Pérez-Mohedano R, Letzelter N, Amador C, VanderRoest C, Bakalis S. Positron Emission Particle Tracking (PEPT) for the analysis of water motion in a domestic dishwasher. Chemical Engineering Journal. 2015;259:724-736.

[28] Jet Discharge Propulsion [Internet]. Engineeringtoolbox.com. 2019 [cited 7 December 2019]. Available from: https://www.engineeringtoolbox.com/jet-discharge-propulsion-force-d_1868.html